CFD MODEL OF WALL BOILING CONSIDERING THE BUBBLE SIZE DISTRIBUTION

E. Krepper[1], R. Rzehak[1], C. Lifante[2], Th. Frank[2]
[1] Helmholtz-Zentrum Dresden-Rossendorf, Germany, E.Krepper@hzdr.de
[2] ANSYS Germany GmbH

ABSTRACT

New developments in the framework of a common project simulating subcooled boiling are described. The computational model used combines the Euler / Euler two-phase flow description with heat flux partitioning. Main achievements are a comprehensive study of the boiling process itself and a better description of the interfacial area by coupling of wall boiling with a population balance model. The paper presents validations and shows the capabilities of the model extensions. A careful calibration of correlations used in the wall boiling model is necessary to obtain agreement with the measured data. For the demonstration, DEBORA tests are used. During these tests radial profiles for gas volume fraction, gas velocity, liquid temperature and bubble size were measured.

1. INTRODUCTION

For engineering calculations, currently the most widely used CFD approach to model two-phase flows with significant volume fractions of both phases is the Eulerian two-fluid frame-work of interpenetrating continua. In this approach, balance equations for mass, momentum and energy are written for each phase, i.e. gas and liquid, separately and weighted by the so-called volume-fraction which represents the ensemble averaged probability of occurrence for each phase at a certain point in time and space. Exchange terms between the phases appear as source / sink terms in the balance equations. These exchange terms consist of analytical or empirical correlations, expressing the interfacial forces as well as the heat and mass fluxes, as functions of the average flow parameters. Since most of these correlations are highly problem-specific, their range of validity has to be carefully considered and the entire model has to be validated against experiments.

For the case of boiling flows, where heat is transferred into the fluid from a heated wall at such high rates that vapour is generated, additional source terms describing the physics of these processes at the heated wall have to be included. A CFD wall boiling model implemented in CFX following the lines of Kurul & Podowski (1991) was calibrated and validated by several authors for other test cases.

Essential for modelling the momentum, mass and energy exchange between the phases is an adequate description of the interfacial area or respectively the bubble size. In the present work a population balance approach coupled to a wall boiling model is used, where bubbles are generated at the wall with a certain size that subsequently evolves due to both coalescence / fragmentation and condensation / evaporation processes.

The model developments were presented by Rzehak et al. (2012). Before the capabilities of this model approach are demonstrated, a careful calibration of correlations used in the wall boiling model is necessary to obtain agreement with the measured data.

2. THE INVESTIGATED EXPERIMENTS

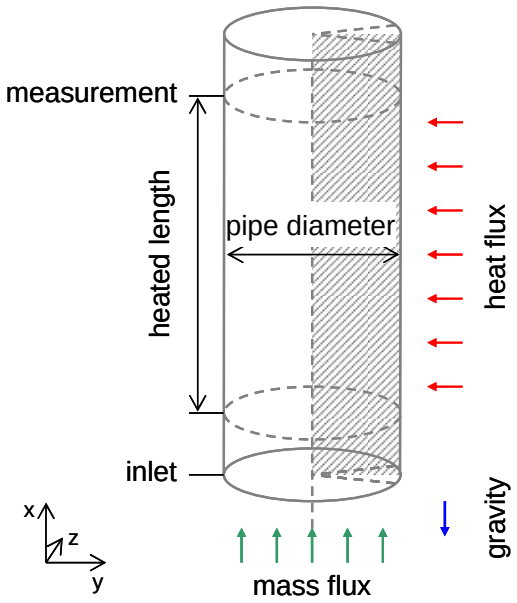

Figure 1: Sketch of the DEBORA test geometry.

A detailed description of the DEBORA test facility can be found in Garnier et al. (2001). In a vertical heated pipe having an inner diameter of 19.2 mm Dichlorodifluoromethane (R12) is heated over a pipe length of 3.5 m as sketched in Fig. 1. The replacement of water by R12 allows measurements at more convenient pressures and temperatures with consistent values for pipe Reynolds number and liquid–gas density ratio. Also advantageous is the possible increase of pipe diameter which enables the measurement of radial profiles. The facility is operated with mass flow rates of 2000 to 3000 kg/m2/s at a system pressure of 1.46 to 2.62 MPa. The radial profiles for gas volume fraction and gas velocity at the end of the heated length are measured by means of an optical probe. Furthermore, profiles of bubble size at this position are determined. In addition, radial liquid temperature profiles as well as axial profiles of the wall temperature are measured by thermocouples.

Table 1: System parameters for the selected test cases, G = 2000 [kg m^{-2} s^{-1}]

	Pressure [MPa]	Wall heat flux [kW m^{-2}]	Inlet subcooling [K]	Inlet tempe-rature [°C]	outlet equilibrium vapour quality
P15-G2-Q76-T30	1.46	76	29.6	28.5	-0.0279
P15-G2-Q76-T27			26.9	31,2	-0.0071
P15-G2-Q76-T23			22.5	35.6	0.0319
P15-G2-Q76-T18			18.4	39.7	0.0687
P15-G2-Q76-T14			13.9	44,2	0.1091
P26-G2-Q74-T28	2.62	74	27.6	58.3	-0.0719
P26-G2-Q74-T26			25.7	60.8	-0.0205
P26-G2-Q74-T20			19.8	66.6	0.0324
P26-G2-Q74-T18			17.9	68.5	0.058
P26-G2-Q74-T16			15.7	70.7	0.0848

Two series of the DEBORA tests have been selected where the inlet temperature increases at otherwise constant conditions (see Tab. 1). The increasing inlet temperature corresponds with a decreasing subcooling and an increasing vapour quality or void fraction. For the series P15-G2-Q76-Txx a shift of the radial gas volume fraction profile from wall peaking (P15-G2-Q76-T30) to core peaking (P15-G2-Q76-T14) was determined in the experiments. For the series P26-G2-Q74-Txx such a shift has not been observed and the profile remains wall peaked. The question is, whether these tendencies found in the tests can also be reproduced in the simulations.

3. THE MODELS

The general equations for diabatic two-phase flow in the Euler/Euler framework of interpenetrating continua have been reviewed in many places before. Therefore, we here focus on those issues that are particularly relevant for the present investigation. The CFX wall boiling model closely follows the heat flux partitioning approach of Kurul & Podowski (1991). It has been emphasized in Krepper & Rzehak (2011) that some of the commonly used correlations are not universally applicable but have to be recalibrated carefully to the specific conditions under investigation. The basis on which such a recalibration can be carried out for varying conditions is discussed. The final outcome of the calibration will be presented in section 4.2.

A second issue is the modelling of interfacial area that determines the exchange of mass, momentum and energy between the phases. For the bubbly flow regime it is convenient to use an equivalent Sauter diameter and work with the bubble size. Obviously, in boiling flows the bubble size may change due to both condensation / evaporation and bubble coalescence / breakup. The importance of taking into account the latter processes has been shown in Krepper & Rzehak (2011). This may be achieved by a population balance model with a source at the wall, the size of the generated bubbles being given by the bubble detachment diameter as calculated from the wall boiling model. Since the rates for bubble coalescence and breakup depend sensitively on the turbulence, bubble induced contributions to the turbulence have to be included as well. To simplify matters, the vapour bubbles are assumed to be at saturation temperature everywhere which is a rather good approximation except close to the critical heat flux.

Turbulent fluctuations are modelled by a shear stress turbulence (SST) model according to Menter (1994), applied to the liquid phase. This corresponds to a $k - \omega$ model near the walls and a $k - \varepsilon$ model far from walls. The frequently used prescription of Sato (1981) for the bubble induced turbulence has been replaced by including source terms in the turbulence equations following Politano et al. (2003). In addition, a wall function for boiling flows based on analogy to a rough wall is employed, which could be shown in Krepper & Rzehak (2011) to give an improved prediction of the velocity profiles.

For momentum exchange between the phases, finally, lift and turbulent dispersion forces are included in the model in addition to the ubiquitous drag force. There is in addition also a force that pushes a bubble translating in an otherwise quiescent liquid parallel to a wall in close proximity away from this wall. Different models for this so-called wall force were investigated but the influence turned out to be small. Therefore in the present study this force was neglected.

4. MODEL SETUP

The models described in the previous section present a rather general framework that can be specialized to the simulation of any subcooled flow boiling problem. The necessary specifications to

simulate the DEBORA test cases will now be described. These comprise prescription of flow domain and boundary conditions, specification of grid and bubble classes as well as calibration of model parameters.

4.1 Geometry and boundary conditions

The tests were simulated in a quasi-2D cylindrical geometry, i.e. a narrow cylindrical sector with symmetry boundary conditions imposed on the side faces. The validity of this simplification has been verified by grid resolution studies and by comparison to a 3D simulation representing a 60° sector of the pipe.

An inlet condition was set at the bottom. The inlet profile for the liquid flow was set according to a typical turbulent flow profile in a pipe. At the outlet at the top a pressure boundary condition was imposed.

All of these two phase flow simulations have been carried out on a quite coarse grid for which the centre of the grid cells adjacent to the wall has a non-dimensional coordinate of y+ ≈ 200. For the test P15-G2-Q76-T27 a grid refinement study was performed which showed no change of the results until this value of y+ has decreased to about 70. For still smaller values no convergence could be achieved. This is a well-known problem of the Kurul and Podowsky (1991) wall boiling model where all vapour generation occurs in the grid cell adjacent to the wall.

4.2 Calibration of parameters

4.2.1 Wall boiling model

The necessity to recalibrate the boiling model parameters to the working fluid and heating surface of the experiment was discussed in a previous study (Krepper & Rzehak, 2011).

For the model of bubble detachment size we proceed as follows. The outermost measurement points of the experimental bubble size profiles are taken as representative of the detachment size. The liquid subcooling at the measurement location is determined from the averaged measured liquid temperature profile. The resulting points were fitted to a correlation given by Tolubinsky and Kostanchuk (1970) for water at different pressures and subcoolings:

$$d_W = d_{ref} e^{-\frac{T_{sat}-T_L}{\Delta T_{redf}}} \tag{1}$$

The adapted parameters for d_{ref} and ΔT_{ref} are given in Tab. 2. Within a pressure level no further calibrations were performed. Rzehak & Krepper, (2012) have applied this procedure to a larger set of test series from which it may be seen that the calibration parameters depend on the flow rate but not on the heat flux.

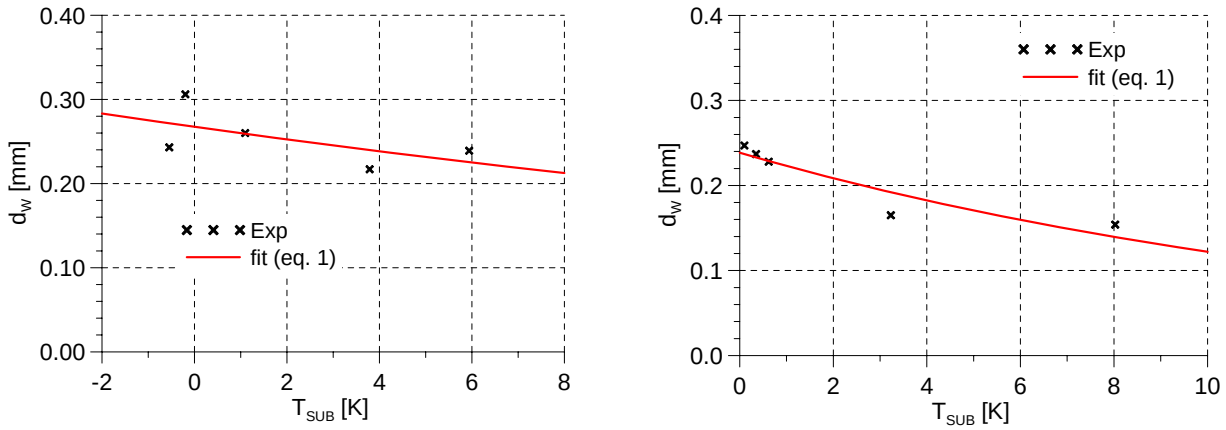

a) P = 1.46 MPa b) P = 2.62 MPa

Figure 2: Bubble size at detachment fitted to measurements

The calibration of the model for nucleation site density is possible by matching the measured axial profiles of wall superheat by calibrating the parameters of the correlation

$$N = N_{ref}\left(\frac{T_W - T_L}{\Delta T_{refN}}\right)^p \qquad (2)$$

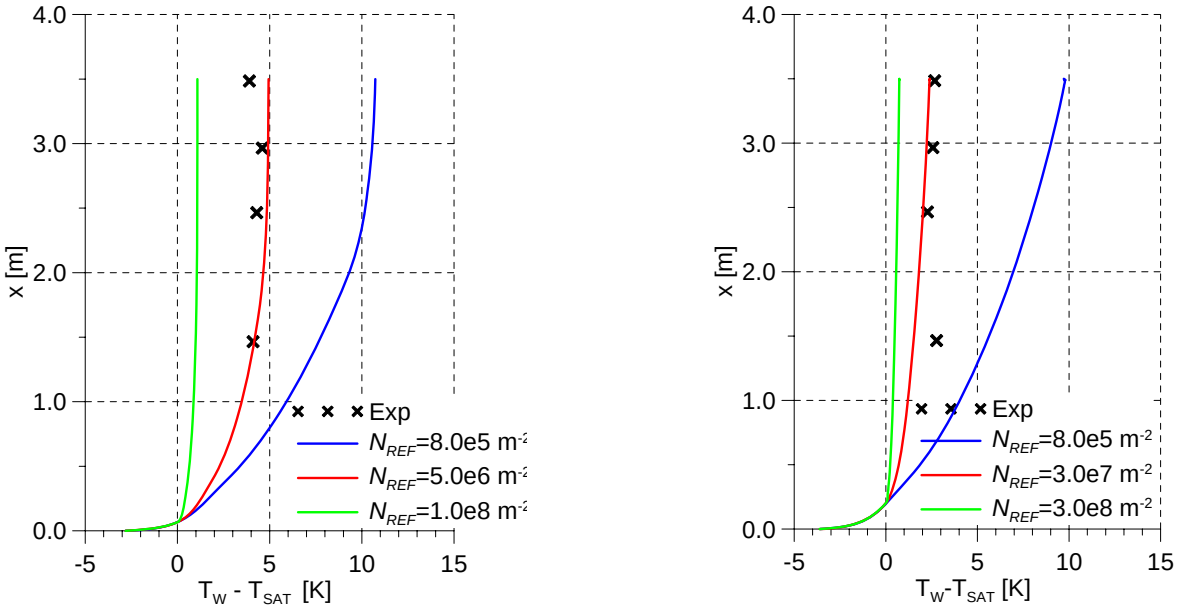

a) Test P15-G2-Q76-T27, P = 1.46 MPa b) Test P26-G2-Q74-T26, P = 2.62 MPa

Figure 3: Wall superheat depending on the reference nucleation site density N_{ref}

Here the nucleation site density may be expected to depend on parameters subcooling, flow rate and heat flux only indirectly through the wall-superheat. Moreover, the sensitivity of the final results with respect to the exponent p = 1.85 is rather low, so only the prefactor N_{ref} will be adjusted for a value of

the reference temperature ΔT_{refN} = 10K. Wall temperature profiles for the selected tests are shown in Fig. 3. A value of $Nref$ = $5.0 \cdot 10^6$ m^{-2} respective $3 \cdot 0.10^7$ m^{-2} gives good agreement with the respective data.

4.2.2 Coalescence and breakup models

In the present work bubble coalescence and breakup are described by the models proposed by Prince & Blanch (1990) and by Luo & Svendsen (1996). To obtain agreement with the measurements, efficiency factors F_C and F_B were introduced and calibrated to match the measured radial bubble size profiles. Bubble size profiles for selected tests and several values of the calibration parameters F_C and F_B are shown in Fig. 4. A good match could be obtained with F_C =0.5 and F_B =0.02 for the complete series of tests at P=1.46 MPa and F_C =0.5 and F_B =0.0625 for the test series at P=2.62 MPa, respectively. Surprisingly, inside a pressure level no further calibration was necessary. This procedure has to be considered only as a first step to demonstrate the potential of the method. Further improvements are necessary replacing the kernel functions describing all relevant mechanisms of bubble coalescence and breakup.

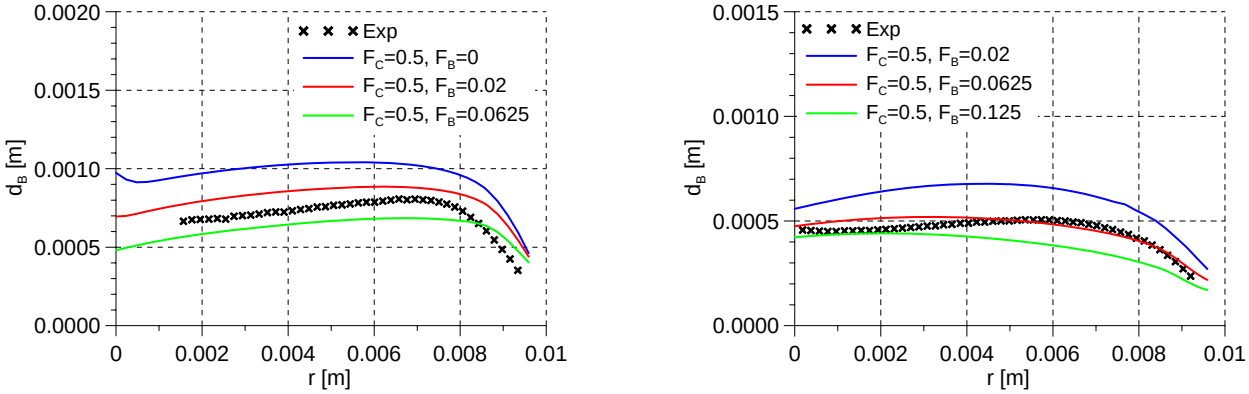

a) Test P15-G2-Q76-T27, P = 1.46 MPa b) Test P26-G2-Q74-T26, P = 2.62 MPa

Figure 4: Measured and calculated radial bubble size profile for different tests

Table 2: Adapted parameters for different test series							
Tests	T_{sub}	Eq. (1) Fig. 2		Eq. (2), Fig. 3		F_C	F_B
		d_{ref}	ΔT_{refd}	N_{ref}	ΔT_{refN}	Fig. 4	
P15-G2-Q76-Txx	30, 27, 23, 18, 14	0.35	45	5.0e+6	10	0.5	0.02
P26-G2-Q74-Txx	28, 26, 20, 18, 16	0.24	45	3.0e+7	10	0.5	0.0625

5. RESULTS

5.1 Test P15-G2-Q76-T14

Previous models for the bubble size in the bulk used a monodisperse approach with bubble size parametrized by the liquid temperature (Krepper & Rzehak 2011). For this model with the heat source at the wall the liquid temperature and consequently the simulated parameterized bubble size decreases with increasing distance from the wall (Fig. 5c, blue line). In the measured bubble size profiles in contrast, an increase of the bubble size with increasing distance from the wall can be observed. The population balance approach introduced in the present work is able to describe at least the correct trends (Fig. 5c, red line).

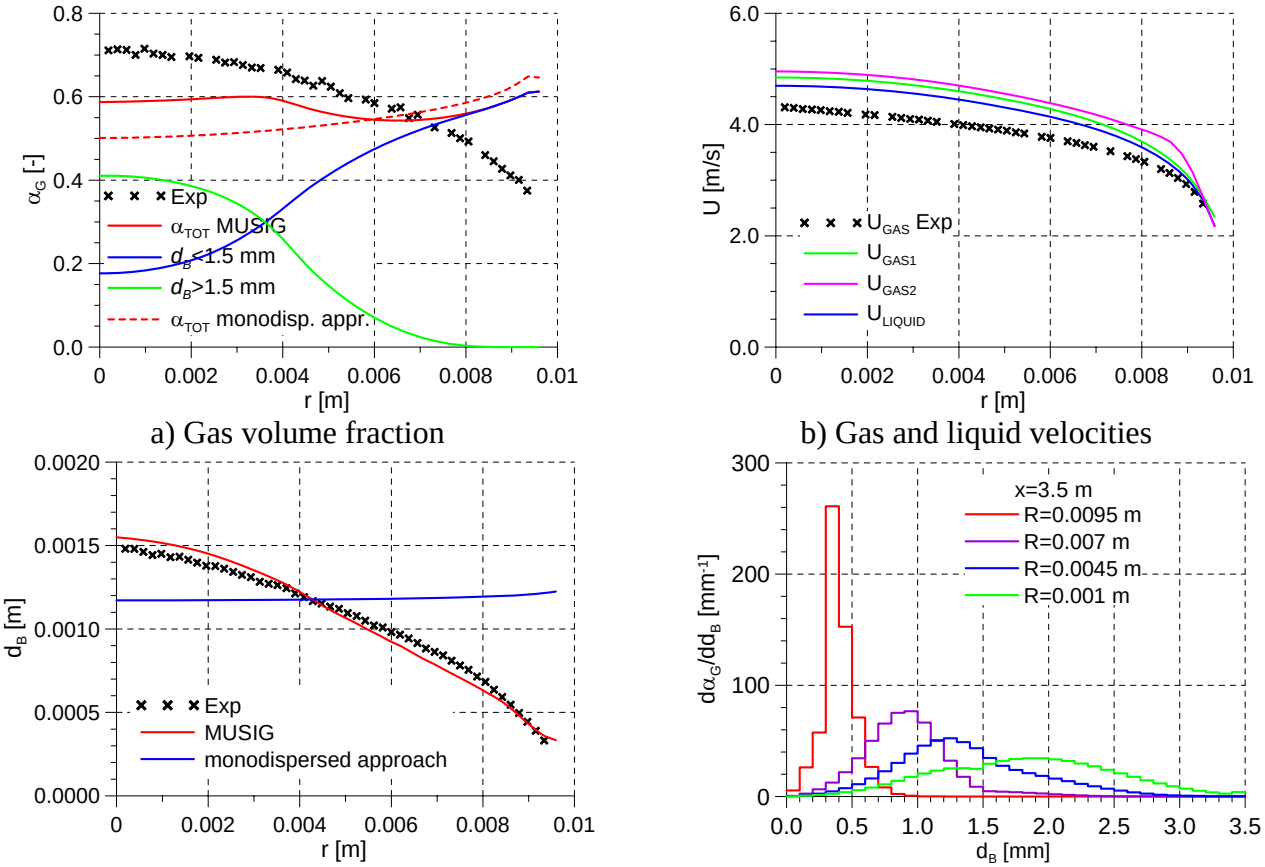

a) Gas volume fraction

b) Gas and liquid velocities

c) Radial bubble size profile

d) Bubble size distribution at three points

Figure 5: Comparison of measured and calculated values for P15-G2-Q76-T14:
P = 1.46 MPa, G = $2 \cdot 10^3$ kg m^{-2} s^{-1}, T_{in} = 35.6 °C

Bubble size distributions are shown in Fig. 5d for four different points at the end of the heated length. The point P1 is located close to the pipe wall, P2 at a wall distance of 0.003 m, P3 at about half of the pipe radius and P4 near the pipe centre. Each point on the curves give the gas volume fraction represented by bubbles of the corresponding size so that the integral over each curve results in the gas volume fraction at the respective location in the pipe. Again, the decreasing gas volume fraction with increasing distance from the wall is evident. At the nearest position close to the wall, P1, a quite narrow

bubble size distribution was found since the bubbles are assumed to leave the heated wall with the detachment diameter d_W. With increased distance from the wall for the points P2 to P4 a shift of the maximum bubble size towards larger values can be observed. Obviously the effect of increasing the average bubble size by coalescence exceeds the effect of bubble shrinking due to condensation. At the same time the size distribution broadens with increasing wall distance.

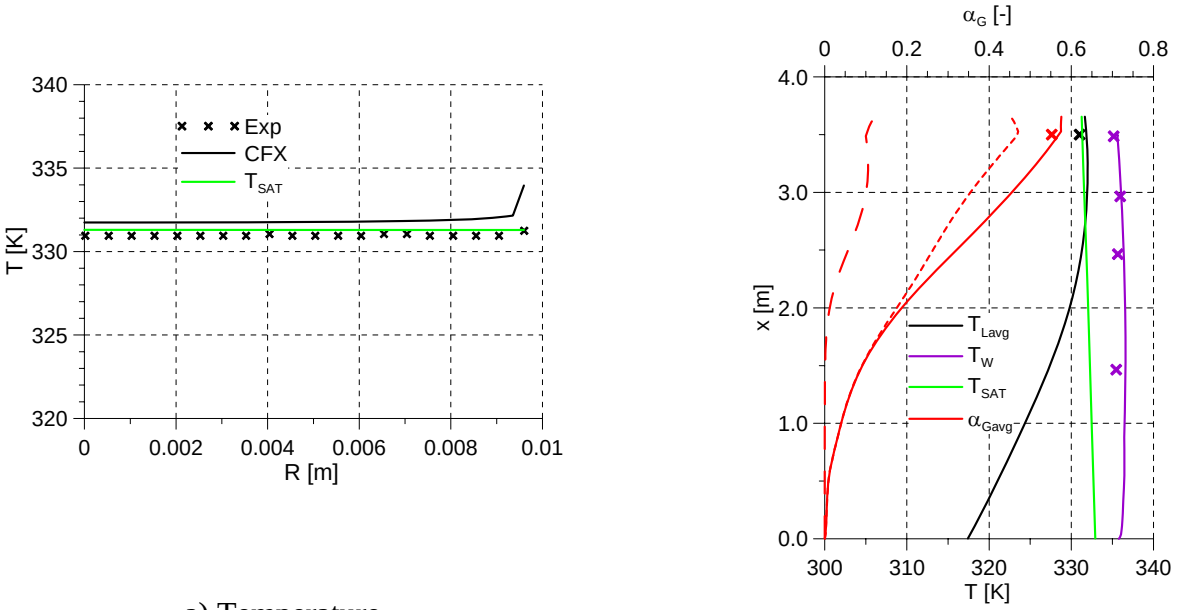

a) Temperature

b) Cross sectionally averaged values

Figure 6: Comparison of measured and calculated values for P15-G2-Q76-T14:
P = 1.46 MPa, G = $2 \cdot 10^3$ kg m^{-2} s^{-1}, T_{in} = 35.6 °C

5.2 Shift of the gas volume fraction profile

Comparing the measured radial gas volume fraction profiles for the test series P15-G2-Q76-T30 to P15-G2-Q76-T14 with increasing inlet temperature respective decreasing subcooling a shift from wall peak to core peak can be observed (see Fig. 7). This phenomenon could not be captured by the monodisperse model approach.

As can be seen in Fig. 7, the models applied here are able to describe the bubble size profiles quite well and at least the tendency of the observed shift of the gas volume fraction maximum is reproduced.

A plausible mechanism transporting the gas towards the pipe center is the lift force which changes its direction for large bubbles. A lift force due to interaction of the bubble with the shear field of the liquid was first introduced to two-fluid simulations by Zun (1980). The corresponding gas momentum source is given by

$$\mathbf{F}^{lift} = -C_L \rho_L \alpha_G (\mathbf{u}_G - \mathbf{u}_L) \times rot(\mathbf{u}_L) \qquad (3)$$

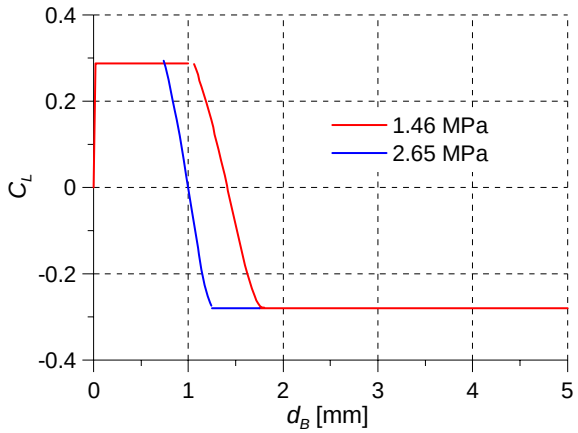

Figure 7: Dependency of the lift coefficient C_L on the bubble size d_B for R12 considering the corresponding material properties

Experimental (Tomiyama et al. 2002) and numerical (Schmidtke, 2008) investigations showed that the sign of C_L changes its sign, if a substantial deformation of the bubble occurs. From the observation of the trajectories of single bubbles rising in simple shear flow of a glycerol water solution a correlation for the lift coefficient was derived. For the water-air system at normal conditions C_L changes its sign at d_B = 5.8 mm which was con-firmed by investigations of polydispersed upward vertical air/water bubbly flow. For R12 this value is decreased substantially to about 1.5 mm at 1.46 MPa and about 1.0 mm at 2.65 MPa, respectively, as shown in Fig. 7.

Indeed, bubbles slightly larger than these values are found in some of the DEBORA tests (see Fig. 5c). This could explain the transport of larger bubbles into the pipe centre.

In the Figs. 8a and b, measured and calculated total gas volume fraction profiles are presented. Fig. 8c and d show the contributions of the individual gas phases representing the different velocity groups. For the group representing the small bubbles (Fig 8c, blue line in Fig. 5a) in all cases a wall peaking profile can be observed due to the lift force pushing these bubbles towards the wall. For the group representing the large bubbles (Fig 8d, green line in Fig. 5a), because of the opposite direction of the lift force, in all cases a radial gas volume fraction profile showing a core peak is observed. With increasing inlet temperature the share of the gas phase representing large bubbles increases and determines the profile shape of the total gas volume fraction.

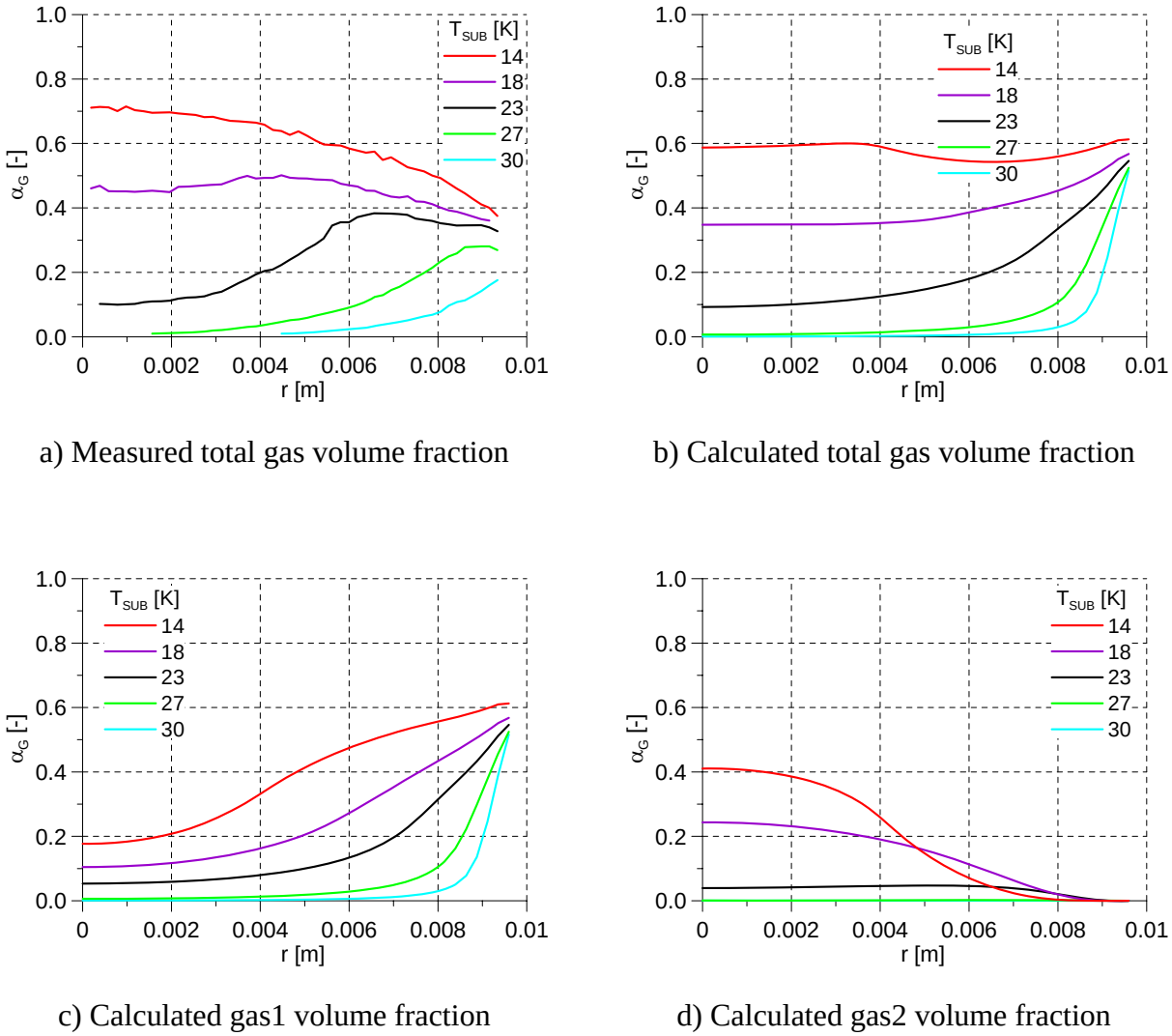

a) Measured total gas volume fraction

b) Calculated total gas volume fraction

c) Calculated gas1 volume fraction

d) Calculated gas2 volume fraction

Figure 8: Measured and calculated radial profiles for gas volume fractions and for bubble size with increasing inlet temperature (P15-G2-Q76-T30 to P15-G2-Q76-T14)

5.3 Parametric variations for the test cases P26-G2-Q74-Txx

In this section, a tests series with varying subcooling for otherwise fixed parameters are compared, namely P26-G2-Q74-T16 to P26-G2-Q74-T28. The resulting changes in the profiles for gas volume fraction, bubble size and liquid temperature at the end of the heated length (x=3.5 m) as the subcooling is varied are shown in Fig. 9, where the left column gives the measured and the right columns the calculated values. The calculated temperature profiles compare quite well with the experimental ones.

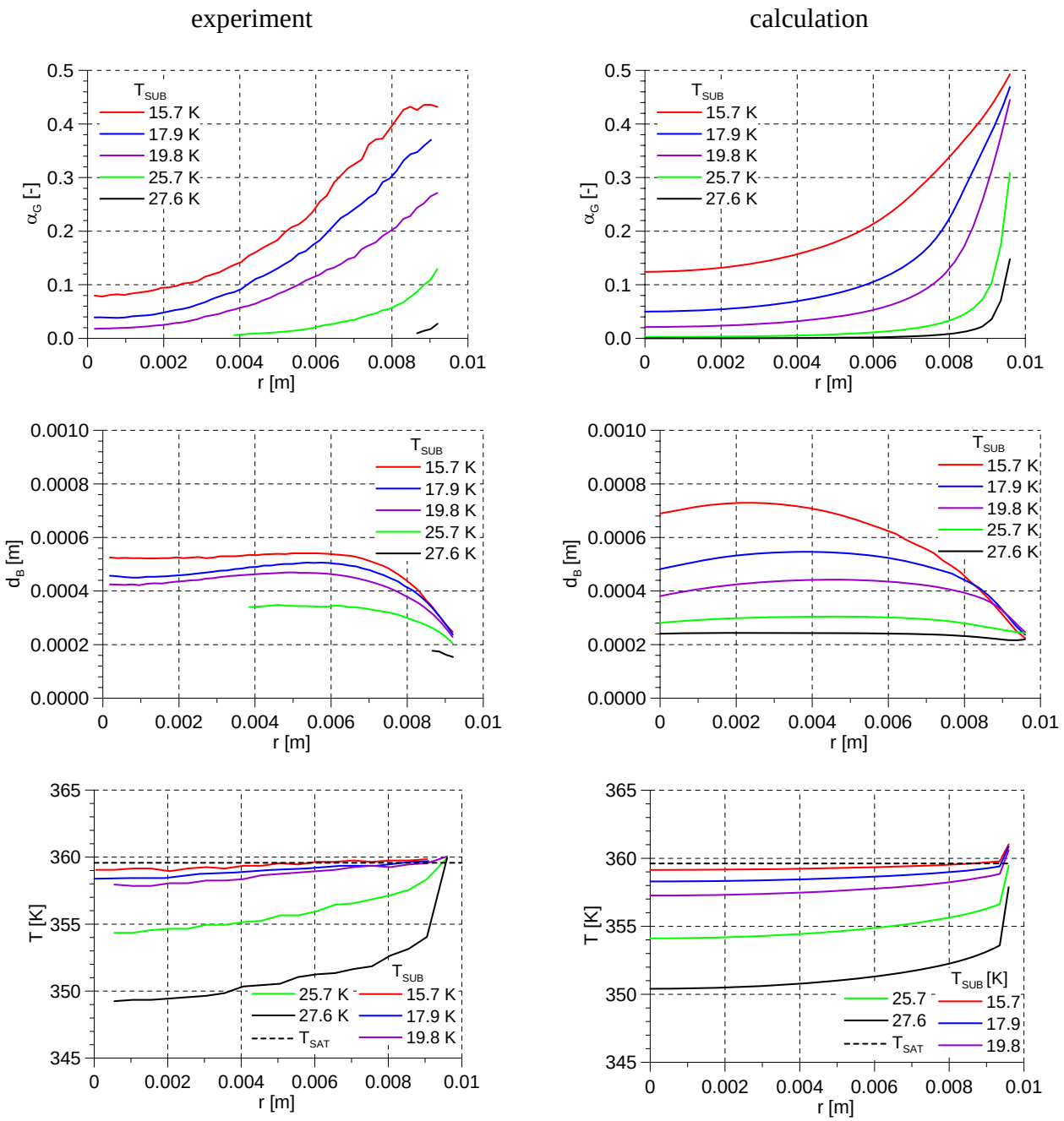

Figure 9: Gas fraction, bubble size and liquid temperature profiles for test series P26-G2-Q74-Txx

For all tests, the bubble size increases with increasing distance from the wall despite the fact that the bulk liquid is subcooled. Clearly this must be due to the coalescence of the bubbles. Again this phenomenon could not be captured by the monodisperse model approach of Krepper and Rzehak (2011). For both test series upon decreasing the subcooling, a strong increase of bubble size is observed in the centre of the pipe while the detachment size changes only relatively little. The present polydisperse modelling approach describes this behaviour at least qualitatively correct. Comparing the radial gas volume fraction profiles with decreasing subcooling, a broadening of the wall peaking profile can be observed for both test series. This effect is due to a lower condensation rate in the bulk liquid as the subcooling decreases. Again this behaviour is described qualitatively correct by the present

modelling approach where bubble of all sizes move with the same velocity. A change from wall to core peaking profiles as for the test series presented in section 5.2 is not observed here. This matches with the explanation that such a transition is related to the sign change in the lift force as discussed in section 5.2. For the presently investigated tests, the bubble size remains below this value while for the actual case of section 5.2 it became larger for the lower values of subcooling.

6. SUMMARY AND CONCLUSIONS

Boiling at a heated wall has been simulated by an Euler / Euler description of two-phase flow combined with a heat flux partitioning model describing the microscopic phenomena at the wall by empirical correlations adapted to experimental data. Such an approach was used previously and adjusted to boiling experiments with water at a pressure of several MPa. Here the applicability and necessary readjustments for similar tests using R12 at the DEBORA facility were investigated. At the same time the bubble size distribution in the bulk was described by a population balance approach by coupling the wall boiling model with the MUSIG model.

A critical review of the detailed correlations used in previous work shows that some of the parameters used in these correlations have to be carefully recalibrated for the present applications. The DEBORA tests provide a large body of information that can be used to this end. Quantities with a strong influence on the amount of produced steam are the bubble size at detachment and the nucleation site density. The former can be taken straight forwardly from the measurements. On the latter unfortunately no direct information is available, however, by matching the temperature of the heated wall, this gap can be closed. In both cases the recalibration results in different values for different pressure levels. It was shown, that for the same pressure condition the parameter set adapted to a certain test can be applied to other tests with equally good agreement.

The measured gas bubble size profiles show an increase of the bubble size with increased distance from the heated wall. A monodispersed treatment is not able to capture this phenomenon but including polydispersity by means of a MUSIG approach and suitable models especially for bubble coalescence this phenomenon can be described. Moreover, a shift of the gas volume fraction profile from a wall peak to a core peak has been observed for a test series with increasing inlet temperature. Again this phenomenon could not be captured by a model with a monodisperse bubble size, but can be described using an inhomogeneous MUSIG approach. Here, bubbles of different size are allowed to move with different velocities and in different directions in response to the bubble size dependent lift force.

A complete polydispersed description requires that processes of coalescence / breakup and condensation / evaporation must be modelled explicitly. For the latter, a suitable model is readily obtained from first principles with the aid of a heat transfer correlation like that of Ranz and Marshall (1952). Unfortunately the former are the more important processes and for these the situation is much less clear. In the present work the commonly applied models for bubble coalescence according to Prince and Blanch (1990) respective for bubble breakup ac-cording to Luo and Svenson (1996) were used as a first step. To reach a fair agreement with the measurements, calibration factors had to be introduced, each valid for a certain pressure level. In this way the suitability of the general model framework could be demonstrated in principle. For a trusted prediction further development of the coalescence and breakup models is necessary.

Finally, looking carefully at the figures showing the gas volume fraction profiles in the near wall region the calculated gas volume fraction is systematically too large. This is particularly evident in the cases

with the pressure of 1.46 MPa. Comparisons with the monodispersed approach show that this effect is not caused by the population balance model. Reasons could be a missing force pushing the bubbles away from the wall or the neglect of swarm effects in the models of drag and lift forces even at gas volume fractions around 50%. Furthermore, the application of the simple heat transfer correlation of Ranz and Marshall (1952) might be questionable. In transferring models used successfully for adiabatic air/water flows to the DEBORA tests it should be noted that bubbles are much smaller here which may require changes beyond simple recalibration of parameters.

Overall, the results confirm the great potential of the Euler / Euler two-phase flow and heat flux partitioning models for the simulation of subcooled flow boiling in industrial applications while at the same time highlighting the need for specific model improvements in order to achieve highly accurate quantitative predictions.

7. ACKNOWLEDGEMENTS

The work was funded by the German Federal Ministry of Education and Research under the contract number 02NUK010A.

8. REFERENCES

Garnier, J., Manon, E., Cubizolles, G. 2001. Local measurements on flow boiling of refrigerant 12 in a vertical tube, *Multiphase Science and Technology*, 13, pp. 1-111

Krepper, E., Rzehak, R., 2011. CFD for subcooled flow boiling: Simulation of DEBORA experiments, *Nuclear Engineering and Design*, 241, 3851– 3866

Kurul, N. & Podowski, M. , 1991: On the modeling of multidimensional effects in boiling channels, *ANS Proceedings of 27th National Heat Transfer Conference*, Minneapolis, MN

Luo, H., Svendsen, H.F., 1996. Theoretical model for drop and bubble break-up in turbulent flows, *AIChEJ*, 42, 5, pp. 1225-1233

Menter, F., 1994, Two-equation eddy-viscosity turbulence models for engineering applications, *AIAA-Journal*, Vol. 32, No. 8.

Politano, M., Carrica, P., Converti, J., 2003. A model for turbulent polydisperse two-phase flow in vertical channels, *International Journal of Multiphase Flow*, 29, 1153

Prince, M.J., Blanch, H.W., 1990. Bubble coalescence and break-up in air-sparged bubble columns, *AIChEJ*, 36, No 10, pp. 1485-1499

Ranz, W.E., Marshall, W.R., 1952, Evaporation from drops, *Chemical engineering progress* Vol. 48 No. 3, pp. 141-146

Rzehak, R., Krepper, E., 2013. CFD for subcooled flow boiling: Parametric Variations, *Science and Technology of Nuclear Installations*, 687494

Krepper, E.; Rzehak, R.; Lifante, C.; Frank, T. 2013. CFD for subcooled flow boiling: Coupling wall boiling and population balance models, *Nuclear Engineering and Design* 255, 330-346

Sato, Y., Sadatomi, M., Sekoguchi, K., 1981. Momentum and heat transfer in two-phase bubble flow-I, *International Journal of Multiphase Flow*, vol. 7, pp. 167-177, 1981.

Schmidtke, M., 2008. Investigation of the dynamics of fluid particles using the Volume of Fluid Method, PhD-Thesis University Paderborn, (in German)

Tomiyama, A., Tamai, H., Zun, I., Hosokawa, S., 2002. Transverse migration of single bubbles in simple shear flows, Chemical Engineering Science, 2002, 57, 1849-1858

Zun, I. 1980. The transverse migration of bubbles influenced by walls in vertical bubbly flow, *Int. J. Multiphase Flow*, Vol. 6, pp. 583-588